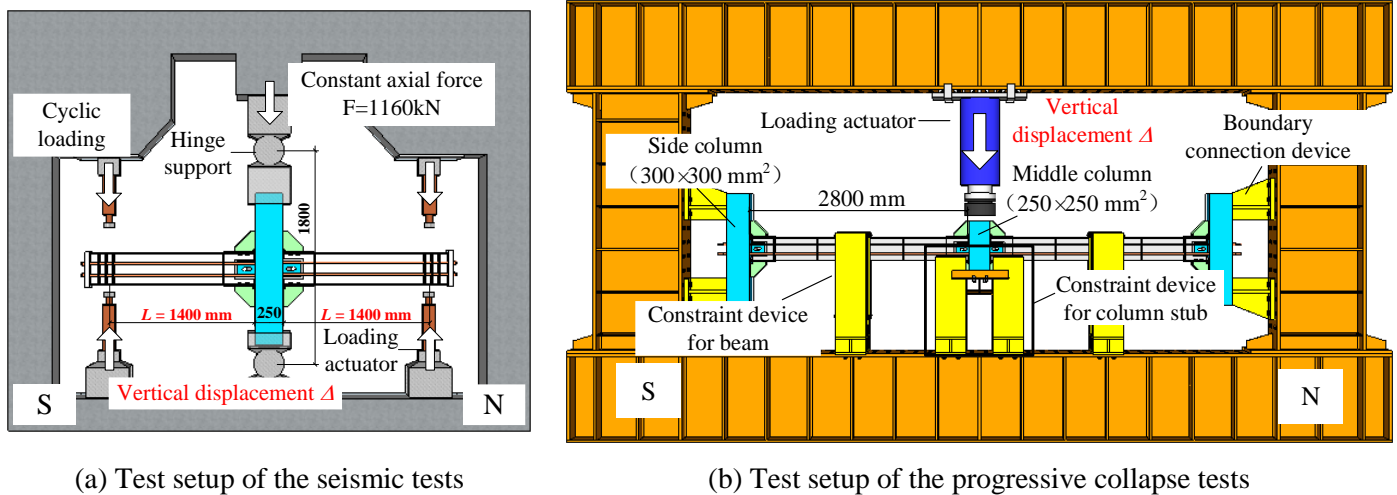




In order to determine a suitable beam sectional dimension for Specimen M-P140-S2, the Specimen M-P140-S1.5 is designed to ensure that the frame beam remains in the elastic stage during the loading. Specimen M-P140-S1.5 was improved on the basis of Specimen M-P100-S. The differences between the two specimens are: (i) The beam sections of Specimen M-P140-S1.5 are strengthened; (ii) the initial pre-stressed level of the PT tendons of Specimen M-P140-S1.5 is improved (from 40% to 52%).

Specimens M-P140-S1.5 and M-P140-S2 were subjected to cyclic loads to evaluate their seismic performance. The corresponding test apparatus is shown in Figure 3a. In the seismic cyclic tests, a constant axial load of 1160 kN was applied vertically at the top of the column for considering the gravity load from the upper stories (Figure 3a). The seismic action is simulated by the cyclic loads at both ends of the beams. The rotation of the beam-column joint (i.e., θ) is calculated by $\theta = \Delta / L$, where Δ is the displacement measured at the beam end and L is the length of the beam. Note that the flexural strength deterioration shall be smaller than 20 % when θ equals 0.04 rad for a composite-special moment frame according to AISC-341-16 [11]. The cyclic loads were measured by the load cells installed at the loading actuators. The internal forces of the PT tendons were monitored by the load cells at the anchorage areas. Moreover, a series of strain gauges were installed on the angle steels and the rib stiffeners and along the beam height to monitor the strain development of different components.

On the other hand, Specimen M-P140-C2, being a two-bay substructure, was subjected to a vertical concentrated load to mimic a middle column removal scenario as shown in Figure 3b. In order to consider the constraint from the peripheral structure, both end columns of Specimen M-P140-C2 were mounted to the steel reaction frame to achieve fix boundaries. The external load was measured by the load cell above the middle column stub. Similar to the seismic cyclic tests, the strain developments and PT tendon forces were also monitored by corresponding instruments. More information about the test setups can be referred to Lu et al. [8].



(a) Test setup of the seismic tests

(b) Test setup of the progressive collapse tests

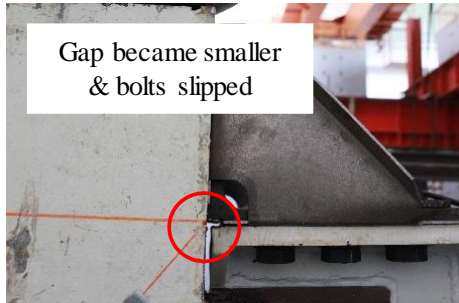
Figure 3. Test setup

3.2 Details of the specimens

The details of Specimens M-P140-S2 and M-P140-C2 are shown in Figures 4a and 5, respectively. The progressive collapse test specimen is of identical dimensions to those of the seismic test specimens at the beam-to-column connection area (Figure 4), therefore similar dimensions are unlabeled in Figure 5. In order to balance the residual bending moment of the replaceable SAS when θ equals 0.04 rad, the initial pre-stress level was set as 52% (i.e., the initial pre-stressed force of a single PT tendon was 140 kN). The details of the SAS in Specimens M-P140-S2 and M-P140-C2 are shown in Figures 4b and 4c.

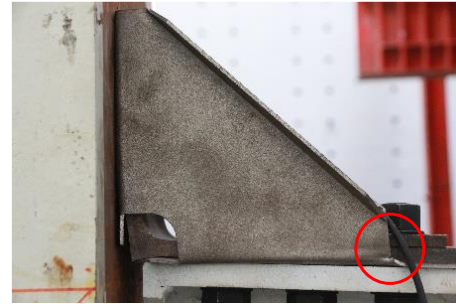


To sum up, SPCRCF-2 demonstrates better seismic and progressive collapse resilience when both the seismic cyclic test results (Section 4.1) and the progressive collapse test results are considered.



Gap became smaller
& bolts slipped

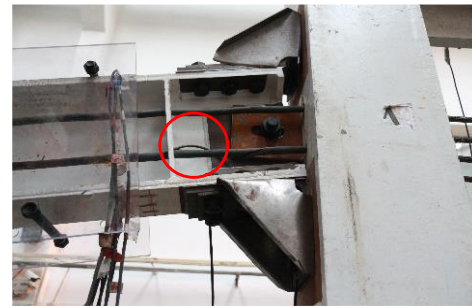
(a) Bolts slipped at Section NE
(1, $\Delta = 53$ mm, $F = 278$ kN)



(b) Tension rib stiffeners began to rupture
(2, $\Delta = 115$ mm, $F = 309$ kN)



(c) Top angle ruptured at Section SA
(3, $\Delta = 372$ mm, $F = 487$ kN)



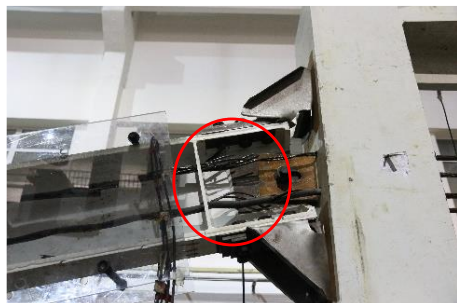
(d) Steel wires of a PT tendon fractured
(4, $\Delta = 389$ mm, $F = 486$ kN)



(e) Bottom angle ruptured at Section NE
(5, $\Delta = 451$ mm, $F = 348$ kN)



(f) Top angle ruptured at Section NA
(6, $\Delta = 496$ mm, $F = 327$ kN)





- (g) Steel wires of PT tendons fractured
(7, $\Delta = 566$ mm, $F = 384$ kN)

Figure 12. Typical phenomena of Specimen M-P140-C2 (Points 1 to 7 refer to Figure 11)

5. Conclusions

In order to improve the seismic and progressive collapse resilience of composite frames, a new composite frame system, namely, SPCRCF-2, is proposed in this study. The performance of SPCRCF-2 is compared with that of the SPCRCF and the CSCCF through seismic and progressive collapse experiments. The primary conclusions are drawn below.

(1) In the seismic tests, Specimen M-P140-S2 could provide similar initial stiffness and yield strength as those of Specimens B-S and M-P100-S. Compared with the conventional frames, the beams and columns in Specimens M-P100-S and M-P140-S2 exhibited no damages, whereas the damage was found on the replaceable SAS components. Consequently, both SPCRCF and SPCRCF-2 exhibited significantly better seismic resilience than conventional frames (CSCCF).

(2) In the progressive collapse tests, the peak strength and ductility of Specimens M-P100-C and M-P140-C2 were higher than those of Specimen B-C. Furthermore, Specimen M-P140-C2 exhibited greater ductility and safety margin compared with Specimen M-P140-C. Additionally, at the end of loading, the key components (beams and columns) of Specimen M-P140-C2 were damage-free. Therefore, SPCRCF-2 exhibited better progressive collapse resilience.

In summary, the proposed new and improved SPCRCF-2 satisfies the seismic and progressive collapse resilience requirements (i.e., large rotation, low damage, self-centering, and easy reparability), and can serve as a reference for future multi-hazard resilient designs of composite frames.

6. Acknowledgements

The authors are grateful for the financial support received from the National Natural Science Foundation of China (No. 51778341) and the Tencent Foundation through the XPLORER PRIZE.

7. References

- [1] National Science Foundation (NSF) (2014): Decision frameworks for multi-hazard resilient and sustainable buildings (RSB).
- [2] Nethercot D, Vidalis C (2015): Improving the resistance to progressive collapse of steel and composite moment frames. *Structures Congress*, 1138-1149.
- [3] Hajjar JF, Leon RT, Gustafson MA, Shield CK (1998): Seismic response of composite moment-resisting connections. II: behavior. *Journal of Structural Engineering*, **124** (8), 868-876.
- [4] Lin KQ, Li Y, Lu XZ, Guan H (2017): Effects of seismic and progressive collapse designs on the vulnerability of RC frame structures. *Journal of Performance of Constructed Facilities*, **31** (1), 04016079.
- [5] Li Y, Ahuja A, Padgett JE (2011): Review of methods to assess, design for, and mitigate multiple hazards. *Journal of Performance of Constructed Facilities*, **26** (1), 104-117.
- [6] Pirmoz A (2011): Performance of bolted angle connections in progressive collapse of steel frames. *Structural Design of Tall and Special Buildings*, **20** (3), 349-370.
- [7] Izzuddin BA, Vlassis AG, Elghazouli AY, Nethercot DA (2008): Progressive collapse of multi-storey buildings due to sudden column loss—Part I: Simplified assessment framework. *Engineering Structures*, **30** (5), 1308-1318.
- [8] Lu XZ, Zhang L, Lin KQ, Li Y (2019): Improvement to composite frame systems for seismic and progressive collapse resistance. *Engineering Structures*, **186**, 227-242.

